Hole mobilities in hydrazone-polycarbonate dispersions

J. X. Mack,* L. B. Schein, and A. Peled
IBM Research Division, Almaden Research Center, 650 Harry Road, San Jose, California 95120-6099
(Received 19 October 1988)

Extensive characterization of the hole mobilities μ in dispersions of *p*-diethylaminobenzaldehyde-diphenyl hydrazone (DEH) in polycarbonate has been carried out. We report the effect of varying the electric field E, temperature T, and spacing between DEH molecules ρ on μ. These data are analyzed by a procedure that allows proper separation of the functional dependencies of the mobility on E, T, and ρ. It is found that $\ln\mu$ is proportional to $E^n(T^{-1}-T_0^{-1})$, where $n=0.5$ and T_0 is a fitted parameter which decreases with increasing ρ, behavior opposite to the dependence of the glass transition temperature on ρ. These experimental results are not yet understood theoretically. Our procedure for separating the ρ and T dependence is applied to data taken on DEH-polycarbonate and to data taken from the literature on another molecularly doped polymer system, *N,N'*-diphenyl-*N,N'*-bis(3-methylphenyl)-(1,1'-biphenyl)-4,4'-diamine (TPD) in polycarbonate. For DEH-polycarbonate, the activation energy is found to be independent of ρ. In contrast, for TPD-polycarbonate the activation energy is strongly dependent on ρ. Our data suggest that small-polaron hopping is occurring in molecularly doped polymers; this different dependence of the activation energy on ρ is consistent with different small-polaron hopping regimes, adiabatic and nonadiabatic, in these two systems.

I. INTRODUCTION

In the past 15 years there has been much interest in the charge-transport behavior of amorphous organic materials. This interest stems from their practical importance as photoconductors in electrophotography[1] and from their importance to amorphous-materials transport theories. Molecularly doped polymers are an important class of amorphous organics studied, since they allow the study of the effects of all three critical hopping transport parameters, molecular concentration, electric field E, and temperature T, on the mobility μ. In this class of materials, published charge-transport data are not consistent with available hopping theories.[1-3]

The form of the drift mobility μ observed experimentally by most workers[3-7] is

$$\mu=a_0\rho^2\exp(-2\rho/\rho_0)\exp(-\Delta/kT)\times\exp[\beta\sqrt{E}\,(1/kT-1/kT_0)]\,, \quad (1)$$

where a_0 is a constant, ρ is the mean calculated distance between dopant molecules, k is Boltzmann's constant, and ρ_0 and Δ represent, respectively, the wave-function decay length and zero-electric-field activation energy. β and T_0 are parameters fit to the data. The observed activated behavior, exponential dependence on ρ, and the magnitude of μ ($<10^{-4}$ cm^2/V s) suggest a hopping transport mechanism. However, a more detailed analysis of the data reveals several puzzling features. For example, ρ_0, the parameter representing the decay length of the wave function, has been reported[5] to increase with temperature, an unexpected result. The activation energy[3,5] has generally been observed to depend upon ρ. The $\sqrt{E}$ dependence and the T_0 parameter remain unexplained.[4,6] Given these puzzling features of the data, it should not be a surprise that attempts to rationalize the values of Δ and T_0 with molecular properties have not yet been successful.

Many authors[2-7] have recognized that the exponential dependence on the calculated distance between dopant molecules, i.e., hopping sites, and activated behavior suggest several well-known hopping theories such as phonon-assisted hopping, nonadiabatic small-polaron hopping, and hopping over potential barriers between each molecule. Unfortunately, there is no known method to distinguish among these theories and it has not been possible to use the theories to predict ρ_0 and Δ. Further, such theories do not predict how Δ should depend upon ρ or explain the puzzling electric field dependence.

In one attempt to understand the electric field dependence, it was suggested that the T_0 parameter is an artifact of the functional forms chosen for Eq. (1). Bässler[8] suggested that the transport takes place by charges hopping in a Gaussian distribution of energy states approximately 0.1 eV wide at each site, this distribution being produced by the amorphous nature of the material. He predicted for the mobility (using computer simulation, which was verified[9] analytically later) that

$$\mu\propto\exp[-(T_1/T)^2]\exp(E/E_0)\,, \quad (2)$$

where T_1 is a constant and E_0 is proportional to T^2. Besides the unusual non-Arrhenius temperature dependence, this model predicts that if $\ln\mu$ is plotted against T^{-2}, then the lines of constant E will intersect on the vertical axis. This obviates the need for the effective temperature T_0 used in Eq. (1) which is not predicted by any theory. Some authors have reported this result (Refs. 8 and 6, but see Discussion below) while others report the need for a T_0 parameter even if $\ln\mu$-versus-T^{-2} plots are used.[3]

Facci and Stolka,[10] adopting an electrochemical point of view, suggested that charge migration can be described as a small electric field perturbation of a succession of diffusional random-walk electron self-exchange reactions between neighboring oxidized and reduced sites. They derive the field dependence by subtracting the field-influenced rate constants in the reverse direction from the forward direction. They predict

$$\mu \propto \exp(\alpha e\rho E/kT) - \exp[-(1-\alpha)e\rho E/kT] , \quad (3)$$

where α is a free parameter between 0 and 1 characterizing the asymmetry of the barrier for forward and backward hops, and e is the electron charge. Equation (3) generalizes the result obtained earlier by Bagley[11] and Seki[12] (in which $\alpha=1$) and has been fitted to hole-transport data in the TPD-polycarbonate system. However, we have found (unpublished) that the TPD-polycarbonate data also can be described by Eq. (1); this occurs because the small reported range in the measured μ makes it difficult to distinguish among various functions proposed.

The $\sqrt{E}$ dependence is predicted by the Poole-Frenkel effect, the lowering of a Coulomb barrier by an applied electric field. Indeed, the magnitude of β in Eq. (1) is observed experimentally to be within a factor of 2 of the value predicted by the Poole-Frenkel theory. This theory has no adjustable parameter, unlike Eqs. (1)–(3). However, most workers[3–6] dismiss this explanantion based on the required unreasonable number of charged impurity centers needed in the polymer film to create the effect. Another suggestion for rationalizing the $\sqrt{E}$ dependence is that the holes may tunnel[7] through, instead of hop over, the Coulomb barrier. This idea also requires the presence of a high concentration of charged impurity centers. Attempts to deal with this objection include postulating self-induced Coulomb wells.[7]

As can be seen, significant questions remain concerning the details of the hopping mechanism in molecularly doped polymers. The work reported here was initiated for two reasons. First, complete characterization of molecularly doped polymer systems has been reported only in a few systems.[3–5,7] Increasing this number should be useful in determining those aspects of the transport behavior which are universal to this class of materials and which are specific to the molecular structure. Second, an obvious prerequisite for identifying the correct hopping mechanism is to properly identify from the experimental data the functional dependencies of the mobility on the electric field, temperature, and molecular concentration. This is complicated by the fact that the variables appear in several of the functions. In a previous study of DEH-polycarbonate[6] an approach was introduced to systematically deconvolute the electric field and temperature dependencies at a constant molecular concentration. The second purpose of this work then is to extend this approach to include the functional dependence of the mobility on the molecular concentration.

The experimental procedures are discussed in Sec. II. The new graphical procedure which we introduce that allows proper separation of the functional dependencies of the mobility on E, T, and ρ is discussed in Sec. III. This procedure is applied to DEH-polycarbonate in Sec. IV and the results are discussed in Sec. V.

II. EXPERIMENTAL PROCEDURE

These studies were performed on the system *p*-diethylaminobenzaldehyde-diphenyl hydrazone (DEH) doped into bisphenol-*A*-polycarbonate (M60 obtained from Mobay Chemical Corporation) at molecular concentrations from 10% to 90%. The structures of these molecules are shown in Fig. 1. The solutions were made by dissolving 10% polycarbonate into HPLC-grade tetrahydrofuran and then adding appropriate amounts of DEH. 75-μm films were coated using doctor blade techniques onto the Al side of semitransparent aluminized Mylar and then covered in order to slow the evaporation for a more uniform coating. The films were dried in a vacuum oven slightly above room temperature for 48 h. The thickness of the dried films ranged from 10 to 50 μm, but were typically 20 μm. The 10–70 % DEH concentration samples were obtained as amorphous films. The 90% DEH samples dried into a polycrystalline films as cast; they were then melted on a hot plate and quenched in air into the amorphous phase. Melted and quenched 100% DEH samples crystallized rapidly at room temperature, and so were not used. The glass transition temperature T_g was measured by differential scanning calorimetry (DSC) and the results as a function of DEH concentration or ρ, the spacing between molecules [Eq. (4) below] are shown in Fig. 2.

The drift mobility was measured using the standard time-of-flight technique. The sample is a capacitor in an *RC* circuit. A charge sheet is photogenerated in the sample by pulsing a 9-mJ, 10-ns, 337-nm (Molectron UV24) nitrogen laser through the semitransparent Al electrode. The laser pulse was absorbed in the first 1 μm of the 10%

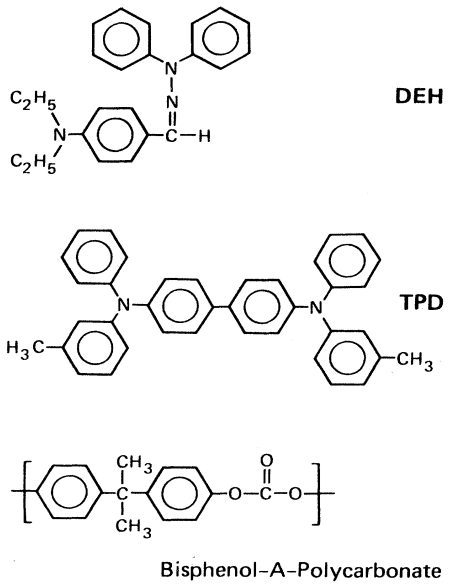

FIG. 1. Structures of the molecules discussed in this paper. DEH and TPD are molecules which are dispersed in polycarbonate to form a thin ($\approx$20 μm) film.

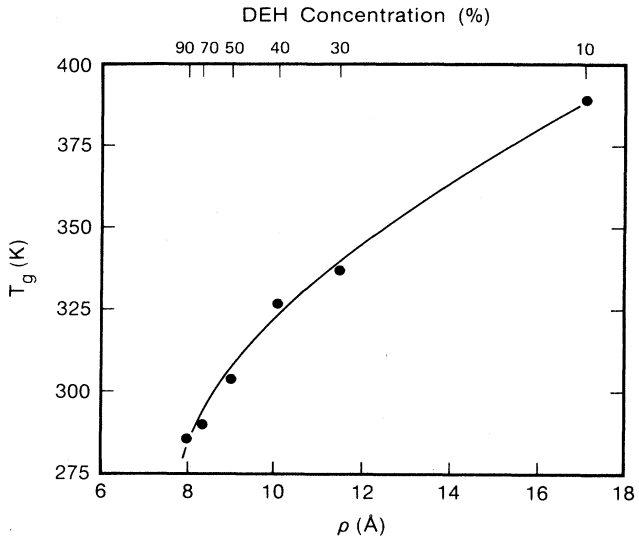

FIG. 2. The glass transition temperature T_g of the DEH-polycarbonate dispersions as a function of DEH concentration and ρ, the mean center-to-center distance between molecules [see Eq. (4)].

DEH sample and at even smaller depths for higher DEH concentrations. The counterelectrode was made by evaporating 100 Å Au over 200 Å SiO. A small patch of Al, 2000 Å thick, was evaporated over the Au for electrical contract. The SiO was necessary to ensure reliable blocking contacts above room temperature. The current transients were collected by a Data Precision 6000 Waveform Analyzer interfaced to an IBM PC computer. All transit times were measured on linear-linear current-versus-time scales, an example of which is shown in Fig. 3. Reproducible "shoulders" could be clearly indentified, indicating

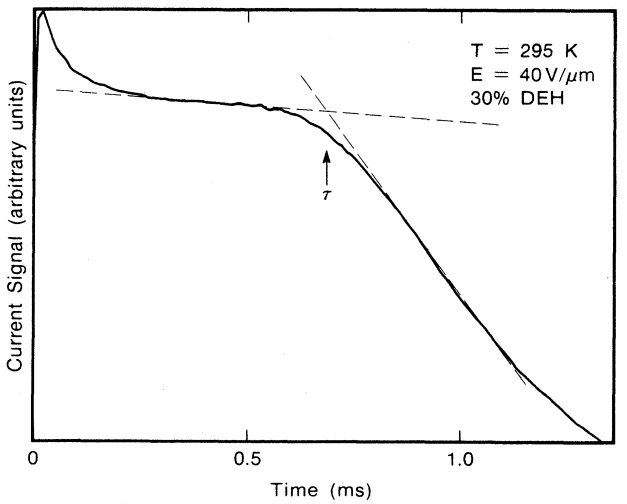

FIG. 3. A current transit waveform after capture and expansion using the Data Precision 6000. Note the clear evidence for a "shoulder" on linear-current linear-time axes, which represents the nondispersive transport time of the holes across the film, used to obtain the drift mobility.

nondispersive transport of the charge packet through the samples. The shoulder identifies the transit time τ which is related to the drift mobility through the relation $\tau=L^2/\mu V$, where L is the thickness of the sample and V is the voltage across the sample. No dependence of the mobility on the excitation light intensity or sample thickness (from 12 to 55 μm) was observed within experimental error.

At each concentration, typically two or three samples from different films were measured. Good reproducibility was obtained even after the films were cycled through the temperature ranges. Temperature control (± 0.5 K) was maintained in a nitrogen Ransco Model 9350 temperature-test chamber. Typically, data were taken below room temperature first, followed by measurements above room temperature. The room-temperature mobility was usually measured at the beginning, middle, and end of the measurement to verify that the sample's mobility remained unchanged.

Two techniques were used to check the quality of the dispersion, i.e., whether any agglomerations of the DEH molecules exist in the films. First, x-ray scattering measurements were performed on the 10%, 20% and 50% DEH samples. No evidence of agglomeration was seen down to 25 Å. Second, the glass transition temperature T_g dependence on ρ was measured (mentioned above, see Fig. 2). That this is a continuous, smooth function even up to 90% DEH concentration argues for a homogeneous film with no segregation or crystallization of the DEH in the polycarbonate.

The stated concentrations of DEH in the samples are given by the mass of DEH relative to the total mass of the DEH and polycarbonate initially mixed into solution when preparing the samples. The concentration of the 30% sample was checked by spectrophotometric analysis of the film. The results were in agreement to better than 1%.

The distance between dopant molecules ρ was calculated using the method commonly used in this field: assuming each molecule has a cubic shape, the center-to-center distance ρ is given by

$$\rho=(M/A\rho_M C)^{1/3}\ , \tag{4}$$

where M is the DEH molecular weight (343 g/mol), ρ_M is its density (1.12 g/cm^3), A is Avogadro's constant (6×10^{23} molecules/mol), and C is the fractional concentration of DEH in the sample. There are some obvious difficulties using this formula to characterize the hopping distance, including the fact that the molecules are not cube shaped and the hopping distance is probably better described by the distance between the edges of the molecules, ρ_e, which, in the cubic approximation for DEH is given by

$$\rho_e=\rho-(M/A\rho_M)^{1/3}=\rho-8\ \text{Å}\ . \tag{5}$$

III. DATA ANALYSIS

Our goal is to determine the functional dependence of the mobility on electric field E, temperature T, and distance between molecules ρ to facilitate identification of

the hopping mechanism. The method for separating the E and T dependence was discussed in Ref. 6 and the method for separating the T and ρ dependence was discussed in Ref. 13. Here we display the complete deconvolution analysis and apply it to the DEH-polycarbonate system.

All workers, both experimental and theoretical, give for a hopping mobility an expression of the form[2-14]

$$\mu = a_0 \rho^2 e^{f_1(\rho)} e^{f_2(T,\rho)} e^{f_3(E,T,\rho)} , \tag{6}$$

where a_0 is a constant which may depend weakly on T. The first exponential describes the overlap integral; the second, the activation energy; and the third, the electric field dependence of μ. Because the variables ρ, T, and E appear in more than one of the f_i, determining the correct form for f_i is not straightforward. For example, a plot of $\ln\mu$ versus ρ cannot be used to determine f_1, since f_2 and f_3 both can have ρ dependence.

The procedure which we introduce to determine the f_i has three steps.

Step (1). Because E only appears in f_3, the E dependence of μ is determined first by plotting $\ln\mu$ versus a power n of E. The slopes S for temperature as a variable and ρ as a parameter are defined as

$$S(T,\rho) \equiv \left[\frac{\partial \ln\mu}{\partial E^n} \right]_{T,\rho} . \tag{7}$$

The T dependence of f_S is determined first at one molecular concentration. By varying the molecular concentration, the dependence of the parameters characterizing the ρ dependence of S, i.e., β and T_0, is determined.

Step (2). We make the assumption that at $E=0$, $f_3=0$. This is justified by the results found empirically[4-7] and theoretically[2,14] by all workers. This assumption allows us to separate f_1 and f_2 from f_3 by using the extrapolated value of μ at zero field $\mu(E=0)$ to determine f_1 and f_2. $\ln\mu(E=0)$ is now plotted versus T^{-1}. The slope of this curve is the zero-field activation energy. The activation energy's dependence on ρ is obtained from similar curves at different DEH concentrations. This determines f_2.

Step (3). Knowing f_2 and $\mu(E=0)$, f_1 can be obtained by graphically solving Eq. (1) or Eq. (6), i.e., by plotting the following function versus ρ,

$$[\mu(E=0)/\rho^2]\exp(\Delta/kT) , \tag{8}$$

taking into account any ρ dependence of Δ, in a semilogarithmic plot.

This procedure allows a deconvolution of the dependence of the f_i on the three variables ρ, T, and E by graphical techniques. It is useful to keep in mind the limitations of such techniques. One can only guess the functional form based on intuition and hope that the guessed functional form leads to the identifications of the correct hopping theory. But the correct functional form is not necessarily simple, and additional effects may occur over wider ranges of temperature, field, or molecular spacing which may require different functions to describe them.

IV. EXPERIMENTAL RESULTS

We now illustrate this unfolding of the dependence of μ on E, T, and ρ for the DEH-polycarbonate system.

A. The function $f_3(E,T,\rho)$

The electric field dependence of the mobility is determined by plotting $\ln\mu$ versus E^n. This is shown in Fig. 4 with $n=0.5$ for a 30% DEH sample. This is the familiar square-root dependence of Eq. (1) that has been observed by most workers[4,6,7] To demonstrate the good fit of $n=0.5$, we have plotted $\ln\mu$ versus E^n for $n=0.1-0.9$ for the DEH concentrations from 20% to 90%. In all of these plots there is a consistent downward departure of the data from a straight line in the $n \geq 0.7$ plots, and a consistent upward departure of the data from a straight line in the $n \leq 0.4$ plots at low electric fields. We find $n=0.5$ or 0.6 best fits our data.

Having found that the power of the electric field is independent of concentration, the T dependence of f_3 is obtained from the slopes of the curves such as those shown in Fig. 4 at various temperatures. In Fig. 5, the slopes S are plotted versus T^{-1}. A linear least-squares fit is obtained ignoring the data point above T_g, suggesting the following form for the function f_3 at constant concentration:

$$f_3 = (\beta/k)\sqrt{E}\,(T^{-1} - T_0^{-1}) , \tag{9}$$

where β and T_0 are constants obtained from the straight-line linear least-squares fit and k is Boltzmann's constant. Performing this procedure for all measured DEH concentrations determines the dependence of β and

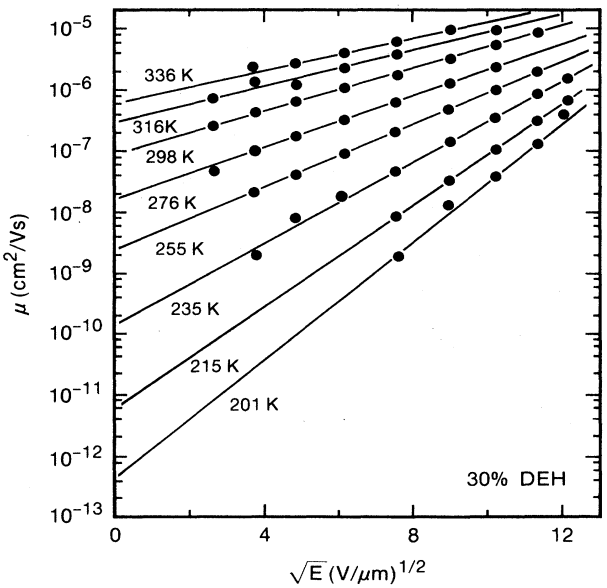

FIG. 4. The data are analyzed by plotting the mobility vs $\sqrt{E}$. The slopes are used to obtain the temperature dependence of f_3 (Fig. 5); the intercepts at $E=0$ are used to obtain f_2 (Fig. 11). The data shown are for 30% DEH which corresponds to $\rho=11.5$ Å.

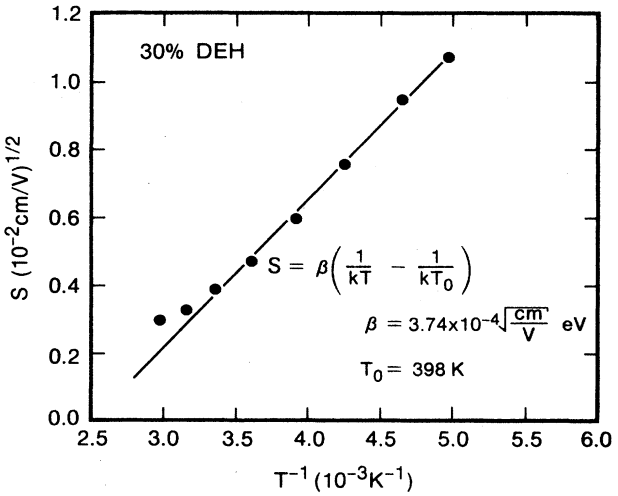

FIG. 5. The slopes of the curves in Fig. 4 are plotted vs T^{-1}. The data, except for the temperatures above T_g, are least-squares fitted to straight line.

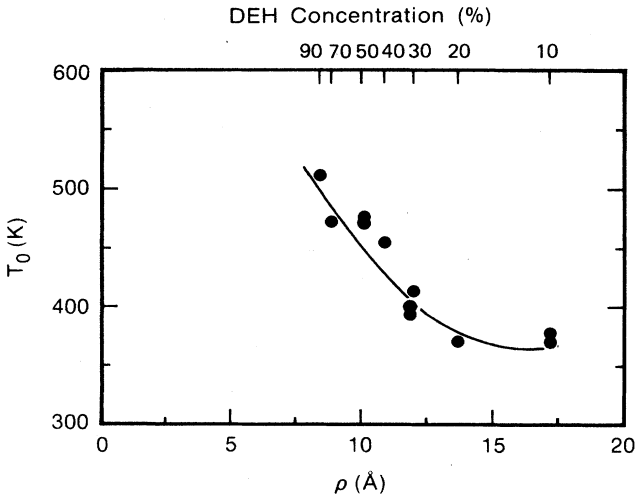

FIG. 7. T_0, obtained from curves such as shown in Fig. 5 at various DEH concentrations from 10 to 90% (ρ=17.2 to 8.3 Å), are plotted vs ρ. T_0 decreases as ρ increases.

T_0 on ρ (Figs. 6 and 7). β appears to increase slightly with ρ while T_0 decreases with ρ.

Two digressions from our procedure are now presented which relate our results to previously published results.[3-5] First, another method of finding T_0, commonly used in the literature, it to note that at $T=T_0$, $f_3=0$, i.e., the field dependence of μ vanishes. Hence, by plotting $\ln\mu$ versus T^{-1} as a function of E, the parameter T_0 can be obtained from the intersection of the curves (Fig. 8). This procedure can give results similar to Fig. 5, but we believe it has more error because of (1) the long extrapolation of many curves, causing a significant difference in the value obtained for T_0 by hand or computer straight-line fits (see below), and (2) the unproven inherent assumption that the temperature dependence of f_1 and f_2 are the same.

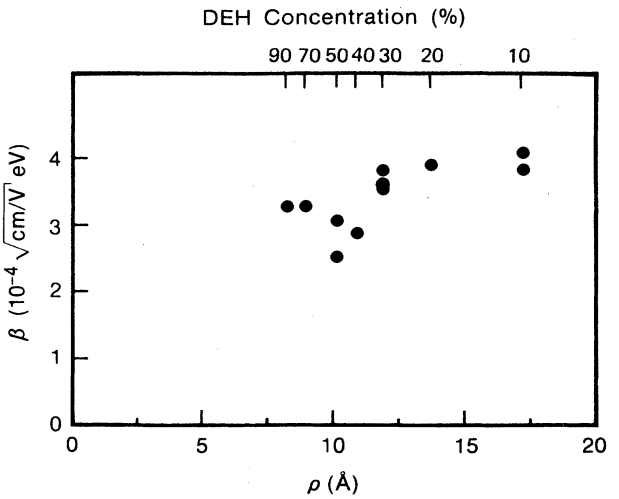

FIG. 6. β, obtained from curves such as shown in Fig 5 at various DEH concentrations form 10−90% (ρ=17.2–8.3 Å), are plotted vs ρ. β is approximately $\approx 3.5\times10^{-4}$ (cm/V)$^{1/2}$ eV.

Second, as mentioned in the Introduction, Bassler[8] has suggested that the unexplained parameter T_0 may be an artifact of the functional form for f_2. He suggested that if $f_2 \propto T^{-2}$, then T_0^{-1} should vanish. In Fig. 9, the same data shown in Fig. 8 are plotted versus T^{-2} and least-squares fitted to straight lines. Our data cannot distinguish whether T^{-1} or T^{-2} is a better fit, but clearly in the T^{-2} plot, T_{02} (which we define as the temperature at which the field dependence vanishes on such plots) is not ∞. In Fig. 10, T_{02}, obtained from plots such as Fig. 9 at each concentration, are shown versus ρ. Obviously, a systematic dependence is seen and T_{02} is not ∞, except perhaps at 90% DEH. (The claim that $T_{02}=\infty$ at 50% DEH-polycarbonate in Ref. 6 was based on hand fits to curves such as Fig. 9. When that data are fitted by least-squares analysis, as is done here, T_{02} is in agreement with present data.) Stolka *et al.*[3] have also found that T_{02} changes with ρ.

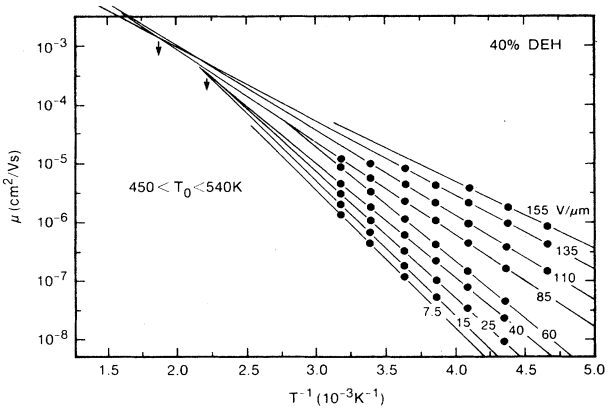

FIG. 8. Another way to obtain T_0 is to plot $\ln\mu$ vs T^{-1} for various electric fields and determine the temperature at which the curves interest, i.e., the field dependences vanishes. For 40% DEH we obtain $450 < T_0 < 540$ K.

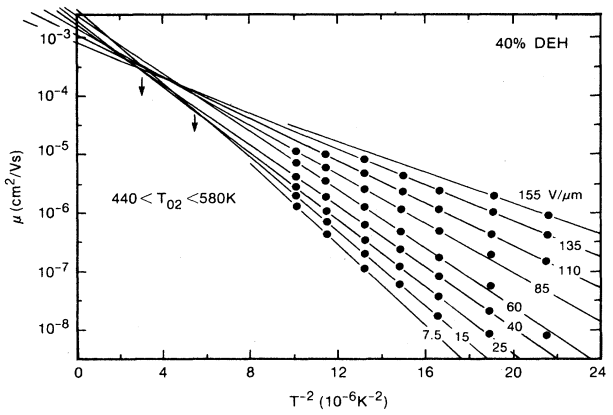

FIG. 9. $\ln\mu$ plotted vs T^{-2} for the various fields as suggested in Ref. 8. The temperature at which the field dependence vanishes, T_{02}, is finite (440–580 K) for 40% DEH.

B. The function $f_2(T,\rho)$

As described in step 2, the temperature dependence of f_2 is found by plotting $\mu(E=0)$ obtained from Fig. 4 as a function of T. Graphical techniques require guessing this function. Two possible choices are T^{-1} and T^{-2}. T^{-2} is a better fit over the whole temperature range, but the data cannot distinguish between T^{-1} and T^{-2} below the glass transition temperature T_g. While T^{-2} was used in previous work[6] on DEH-polycarbonate, the motivation for using T^{-2} has considerably weakened, in view of the data shown in Fig. 10 and recent data given in Ref. 15. Therefore, we choose to use the simpler and more conventional T^{-1} dependence.

To find the activation energy Δ at each concentration and to eliminate the effect of E, T, and ρ dependence of f_3 on Δ, one plots on a semilogarithmic scale $\mu(E=0)$ versus T^{-1}:

$$-\frac{\Delta}{k}=\left[\frac{\partial \ln\mu}{\partial T^{-1}}\right]_{\rho,E=0}. \tag{10}$$

Such a plot for 30% DEH is shown in Fig. 11. The activation energy was determined from the slope of such curves for data below T_g (Fig. 2). The activation energies, plotted as a function of ρ, are shown in Fig. 12. Note that for the DEH-polycarbonate system the activation energy (0.60±0.02 eV) is independent of ρ over the range investigated, in agreement with thermally stimulated current measurements.[16]

As a comparison and to aid later discussions, data taken from the literature[3] on TPD-polycarbonate are also plotted. This is possible because data were published at electric fields low enough that $\mu(E=0)$ could be approximated, a prerequisite of our procedure. Note that in the case of TPD-polycarbonate the activation energy is strongly dependent on ρ, as was shown in Ref. 3.

C. The function $f_1(\rho)$

In prior works, the explicit ρ dependence of the mobility, $f_1(\rho)$, was determined by fitting the mobility data to

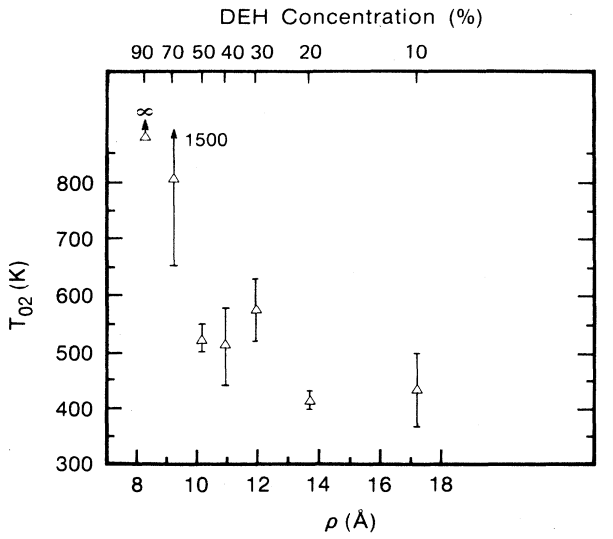

FIG. 10. T_{02}, the temperature at which the field dependence vanishes in plots of $\ln\mu$ vs T^{-2}, are plotted vs ρ. T_{02} decreases as ρ increases.

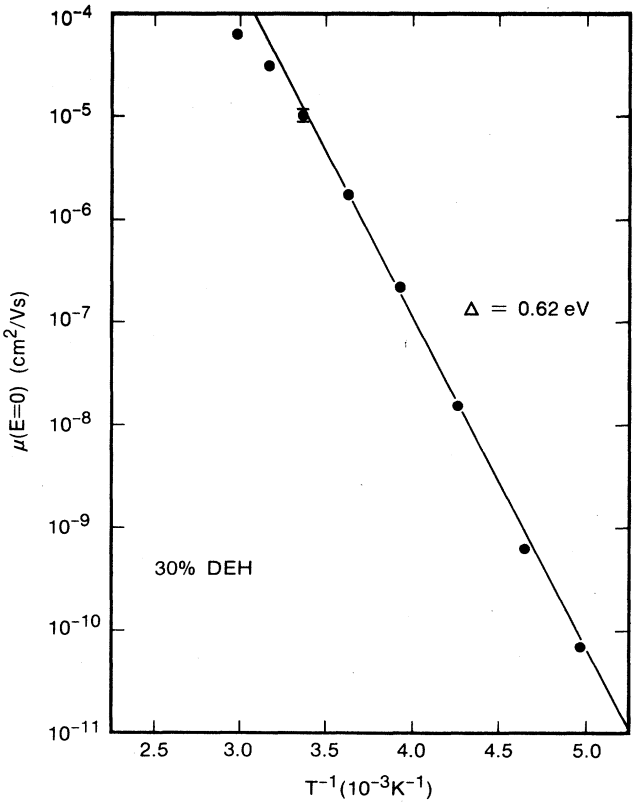

FIG. 11. The intercepts of Fig. 4 [$\mu(E=0)$] are plotted vs T^{-1} to obtain the activation energy Δ. For 30% DEH, $\Delta=0.62$ eV. Data points above T_g were ignored in obtaining the straight line.

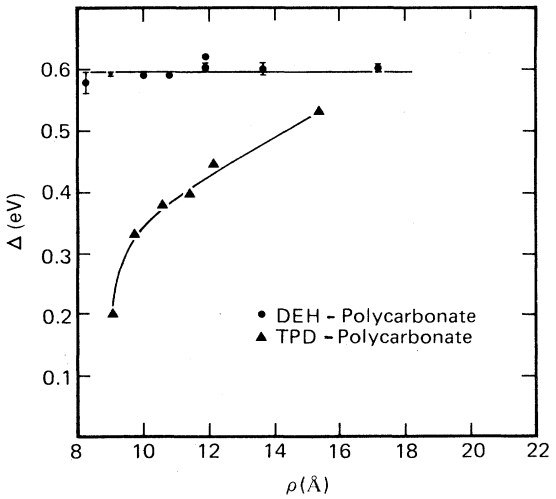

FIG. 12. The activation energies for DEH-polycarbonate obtained from figures similar to Fig. 11 and published data (Ref. 3) for TPD-polycarbonate plotted as a function of ρ. The activation energy for DEH-polycarbonate system is independent of ρ. The activation energy for TPD-polycarbonate system is strongly dependent on ρ. Representative error bars are shown.

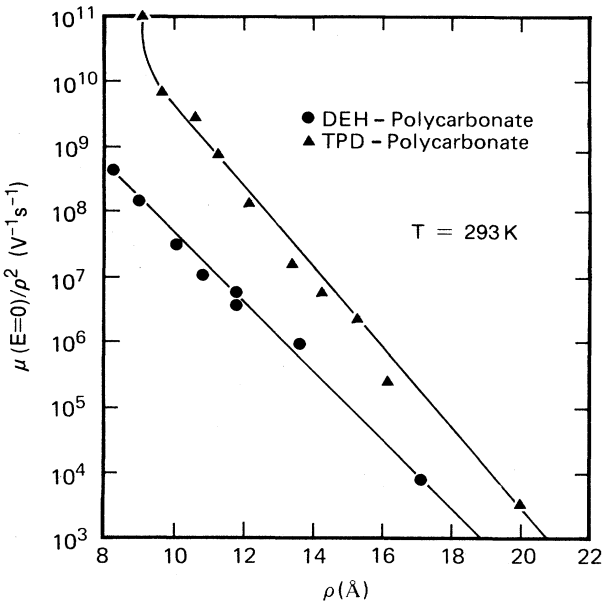

FIG. 13. Semilogarithmic plots of (μ/ρ^2) as in commonly done in the literature for DEH-polycarbonate and literature data (Ref. 3) for TPD-polycarbonate. The mobility chosen was at zero electric field.

the equation

$$\mu \propto \rho^2 \exp(-2\rho/\rho_0) \tag{11}$$

for some arbitrary electric field, where ρ_0 is obtained from the slope of the graphs. This procedure correctly gives the *total* ρ dependence of μ, i.e., the ρ dependence contained in all the functions f_1, f_2, and f_3. It does *not* correctly give the ρ dependence of f_1 alone. This can only be done after first separating out the ρ dependencies of f_2 and f_3. A prior report[5] of a temperature-dependent ρ_0 may have resulted from not properly separating the functional dependencies of μ on ρ. Plots suggested by Eq. (11) for DEH-polycarbonate and TPD-polycarbonate are shown in Fig. 13. In this plot we have used the zero-field value of μ, $\mu(E=0)$, to aid in our deconvolution process, since this eliminates the effects of f_3 on μ. The $\mu(E=0)$ value was obtained by extrapolation (see Fig. 4) for DEH-polycarbonate, and from Fig. 4 of Ref. 3 for TPD-polycarbonate, in which a low enough value of the field was chosen so that the mobility was virtually field independent. The data in Fig. 13 still convolute the functions f_1 and f_2. Deconvolution of f_1 and f_2 is done next.

In step 3 discussed above, it was pointed out that with the functional dependence of the f_2 on ρ determined, one can determine $f_1(\rho)$ by solving Eq. (6) graphically, i.e., solving

$$\mu(E=0)=a_0\rho^2 \exp[f_1(\rho)] \exp(-\Delta/kT) \tag{12}$$

for $f_1(\rho)$. This is done by plotting Eq. (8) versus ρ in Fig. 14, where $\mu(E=0)/\rho^2$ is obtained from Fig. 13 and Δ is obtained from Fig. 12. Figure 14 shows that for the DEH-polycarbonate system, f_1 is exponential in ρ. In contrast, for TPD-polycarbonate, f_1 is independent of ρ except for the data point at 9.2 Å. We ignore this data point in our analysis since it corresponds to 100% TPD and is therefore susceptible to crystallization, or may represent a different hopping mechanism in the absence of polycarbonate.

V. DISCUSSION

Combining the f_i for the two molecules discussed in Sec. IV, we obtain for DEH-polycarbonate

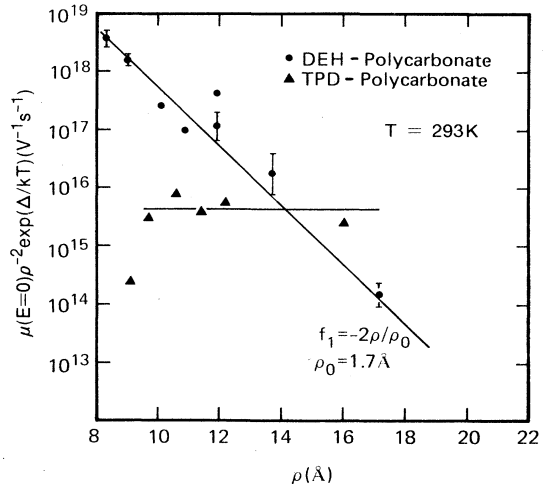

FIG. 14. The dependence of f_1 on ρ can be unfolded graphically by combining the results of Figs. 12 and 13 [see Eq. (8)]. For DEH-polycarbonate f_1 can be described by $-(2\rho/\rho_0)$, consistent with nonadiabatic small-polaron hopping. For the TPD-polycarbonate system f_1 is independent of ρ, consistent with adiabatic small-polaron hopping.

$$\mu = a_0 \rho^2 \exp[-(2\rho/\rho_0)] \exp(-\Delta/kT) \times \exp(\beta\{\sqrt{E}\,[1/kT - 1/kT_0(\rho)]\}) , \quad (13)$$

where

$$a_0 = 1.25 \times 10^{23}\ \mathrm{V^{-1}\,s^{-1}} ,$$

$$\rho_0 = 1.7\ \text{Å} ,$$

$$\Delta = 0.6\ \mathrm{eV} ,$$

$$\beta = 3.5 \times 10^{-4}\ [(\mathrm{cm/V})^{1/2}\,\mathrm{eV}]$$

(see Fig. 6), and the $T_0(\rho)$ are given in Fig. 7. There may be a slight dependence of β on ρ. The zero-field mobility for TPD-polycarbonate is

$$\mu(E=0) = a_0 \rho^2 \exp[-\Delta(\rho)/kT] , \quad (14)$$

where

$$a_0 = 1.2 \times 10^{15}\ \mathrm{V^{-1}\,s^{-1}}$$

and the $\Delta(\rho)$ are given in Fig. 12.

Clearly the observed electric field dependence is not simple. There is a temperature-dependent term and a temperature-independent term associated with T_0. Our data significantly improve the characterization of the field dependence. We have shown the $\sqrt{E}$ is a very accurate description of the data: writing $\ln\mu \propto E^n$, we find that $n \leq 0.4$ or $n \geq 0.7$ are inconsistent with the data. Such a simple result is unexpected in our view, since this field dependence appears to describe two effects, one temperature dependent and one temperature independent. The T_0 parameter, which characterizes the temperature-independent term, has been determined over the full range of molecular concentrations. Plotting T_0 versus ρ (Fig. 7) reveals that T_0 decreases as ρ increases. This is opposite to the behavior of the glass transition temperature (Fig. 2), suggesting that the physical significance of T_0 is probably not associated with rheological properties of the polymeric film.

Despite this new and more detailed information concerning the field dependence of μ, we, along with others, cannot yet suggest any physical mechanism which rationalizes how the electric field affects the hole mobility. Prior attempts to explain the field dependence and objections to these suggestions include the following ideas. (1) The barrier to hopping, the Poole-Frenkel effect,[3,5,6] or tunneling[7] is lowered by the field. As mention in the Introduction, these models require an unreasonable number of charged Coulomb traps in the polymer film. (2) The electric field modifies the energy distribution of final states that the hole can hop to.[8] Computer simulation[9] predicts that $\ln\mu$ is linear in E, not $\sqrt{E}$, as is observed. In addition, this theory predicts $T_{02} = \infty$, which is inconsistent with the data (Figs. 9 and 10). (3) Various kinetic-rate theories[10–12] predict dependencies of $(\sinh E)/E$. This does not fit data on molecularly doped polymers. The modification of kinetic theory introduced by Facci and Stolka[10] needs to be checked over larger ranges of μ and E; this work is in progress.

Inspecting the ρ and T dependence of Eqs. (10) and (11) reveals a striking result: for TPD-polycarbonate, the functional dependence for $\exp[f_1(\rho)]$ is not of the form $\exp(-2\rho/\rho_0)$ but is independent of ρ, while this function does not appear in the expression for μ for DEH-polycarbonate. Further, Δ depends on ρ for TPD-polycarbonate (Fig. 12) but is constant for DEH-polycarbonate. We believe this is a significant clue to the underlying transport mechanism. Since both systems are examples of molecularly doped polymers, it is probable that the same underlying transport phenomena are acting in both cases. Such differences in behavior can currently be united only within the framework of the small-polaron hopping theory,[14] in which the hopping particle is a charge and an associated lattice (molecular) distortion which results from a charge-phonon interaction. In this theory the zero-field mobility is proportional to the product of the frequency of energy-level coincidences of two neighboring hopping sites and the probability P that a small polaron will hop during an energy-level coincidence.

Quantitatively, the mobility of a small polaron in the limit of zero electric field[14] can be expressed as

$$\mu(E=0) = \frac{e\rho^2}{kT} P \frac{\omega}{2\pi} \exp\left[-\frac{E_p/2 - J}{kT}\right] , \quad (15)$$

where E_p is the polaron binding energy and ω is the phonon frequency. In terms of the f_i in Eq. (1),

$$a_0 = \frac{e\omega}{2\pi kT}, \quad \exp(f_1) = P, \quad f_2 = -\frac{E_p/2 - J}{kT} . \quad (16)$$

P represents the probability that a charge carrier will hop once an energy coincidence occurs, the factors after P are the frequency of energy coincidences, and $e\rho^2/kT$ convert a hop frequency into a mobility using the Einstein relation. The activation energy is decreased by the electron overlap J because it broadens the energy levels, decreasing the thermal energy needed to cause an energy coincidence.

Two regimes are predicted by this theory. The probability P and the activation energy have functionally different forms in the two regimes. The adiabatic regime is defined by $P = 1$. In this regime the electron overlap is large enough that a jump is assured whenever there is an energy-level coincidence. Since $J(\rho)$ is large, the activation energy is reduced from the polaron binding energy, i.e., $\Delta(\rho) = E_p/2 - J(\rho)$. The nonadiabatic regime is defined by $P < 1$. In this regime the probability P depends on the overlap integral, $P \propto J^2 \propto \exp[-(2\rho/\rho_0)]$. Also, since J is small, in this case the activation energy is essentially independent of concentration: $\Delta = E_p/2$. In this framework we can now provide a unified picture of the hole-transport mechanisms in DEH-polycarbonate and TPD-polycarbonate systems. The TPD-polycarbonate system exhibits an adiabatic behavior and therefore has an activation energy that depends on ρ and has no prefactor containing the overlap integral. The DEH-polycarbonate system, on the other hand, exhibits the nonadiabatic behavior with a constant activation energy and a prefactor of the form $J^2 \propto \exp[-(2\rho/\rho_0)]$.

Translating the above ideas into microscopic physics associated with the molecules requires an explanation of

why both systems, which cover approximately the same concentration range, 10–90 % should exhibit high-J and low-J regimes, i.e. adiabatic and nonadiabatic small-polaron hopping. A possible answer lies in the fact that the dopant molecules, having lengths of the order 10 Å, have dimensions comparable to the largest values of ρ calculated, and therefore are in close contact, despite the apparent dilution. Because of the different shapes of the TPD and DEH molecules, there will be very different steric hindrances at play, possibly enhancing the overlap of the polaron-carrying portions of the TPD-polycarbonate molecule, while hindering those in the DEH-polycarbonate system. Quantitative comparison of these data to the theory will probably require an extension of the one-dimensional, one-optical-phonon model to a more realistic treatment of the many molecular vibrations which could cause the formation of polarons in this system and the three-dimensional nature of the problem.

While we think that the analysis of the these two systems are strong arguments for the applicability of the small-polaron theory to describe charge transport in molecularly doped polymer systems, it would obviously strengthen the case if a system were found that exhibited a transition in the functional forms of $f_1(\rho)$ and $\Delta(\rho)$ from the adiabatic to the nonadiabatic regimes by varying ρ. It is also possible that the concept of such regimes is not unique to the small-polaron model. For example, Duke and Meyer[17] presented a hopping model in which a ρ dependence of Δ is predicted.

VI. CONCLUSION

Extensive characterization of the hole mobilities in DEH-polycarbonate has been given as a function of the electric field, temperature, and molecular spacing. These data have been analyzed by a new deconvolution procedure which allows proper separation of the functional dependencies of the mobility on E, T, and ρ.

It is found that $\ln\mu \propto E^n$ with $n=0.5$ over the full range of DEH concentrations, from 10–90 %. It is also found that $\ln\mu \propto \beta/k\sqrt{E}\,(T^{-1}-T_0^{-1})$. β appears to increase slightly with ρ, while T_0 decreases as ρ increases. This is the first functional characterization of the ρ dependence of T_0 over a concentration range of 10–90 %. It is found that T_0 behaves opposite to the dependence of glass transition temperature on ρ, suggesting that the physical significance of T_0 is probably not associated with rheological properties of the polymeric film. In plots of $\ln\mu$ versus T^{-2} the temperature at which the field dependence vanishes is not ∞, but varies systematically with ρ, which is inconsistent with the theory suggested in Ref. 8. Despite this new and more detailed information concerning the field dependence of μ, the fits are purely phenomenological and need to be tested over wider electric field ranges, work which is presently in progress.

In contrast to the field dependence, separation of the ρ and T dependence by our new deconvolution procedure has provided significant new information about the mechanism of hole hopping. By this procedure, we have analyzed data from DEH-polycarbonate, and a published system, TPD-polycarbonate, and have shown that the data, after systematic analysis, indicate two basic differences between the two systems. For DEH-polycarbonate, the activation energy is constant versus ρ, and μ has a prefactor exponential in ρ. For TPD-polycarbonate the activation energy is dependent on ρ but μ appears to be otherwise independent of ρ, i.e., there is no evidence for a temperature-independent term such as $\exp(-2\rho/\rho_0)$. Both of these results have been predicted in the polaron literature as the natural consequence of the change from nonadiabatic to adiabatic small-polaron hopping. Thus, we have produced a consistent picture of hopping in molecularly doped polymers despite strikingly different experimental functional dependencies. This association of polaron hopping as the hole-transport mechanism allows for the first time the identification of the important material parameters E_p and J that govern hopping in the molecularly doped polymer systems.

ACKNOWLEDGMENTS

The authors would like to acknowledge the x-ray scattering measurements done by Tom Russell, the glass transition temperature and DEH concentration measurements done by Evelyne Hadziioannou and Bruce Fuller, and critical reading of the manuscript by J. Campbell Scott.

*Present address: Varian Associates, Fremont, CA 94538.

[1]L. B. Schein, *Electrophotography and Development Physics* (Springer, New York, 1988).
[2]J. Mort and G. Pfister, in *Electronic Properties of Polymers*, edited by J. Mort and G. Pfister (Wiley, New York, 1982), p. 215.
[3]M. Stolka, J. F. Yanus, and D. M. Pai, J. Phys. Chem **88**, 4707 (1984).
[4]W. G. Gill, J. Appl. Phys. **43**, 5033 (1972); Mol. Cryst. Liq. Cryst. **87**, 1 (1982).
[5]G. Pfister, Phys. Rev. B **16**, 3676 (1977).
[6]L. B. Schein, A. Rosenberg, and S. L. Rice, J. Appl. Phys. **60**, 4287 (1986).
[7]S. J. Santos Lemus and J. Hirsh, Philos. Mag. B **53**, 25 (1986).
[8]H. Bässler, Philos. Mag. **50**, 347 (1984).
[9]M. Grünewald, B. Pohlmann, B. Movaghar, and D. Wurtz, Philos. Mag. B **49**, 341 (1984).
[10]J. S. Facci and M. Stolka, Philos. Mag. B **54**, 1 (1986).
[11]B. G. Bagley, Solid State Commun. **8**, 345 (1970).
[12]H. Seki, in *Proceedings of the Fifth International Conference on Amorphous and Liquid Semiconductors* (Taylor and Francis, London, 1974), p. 1015.
[13]L. B. Schein and J. X. Mack, Chem. Phys. Lett. **149**, 109 (1988).
[14]D. Emin, in *Electronic and Structural Properties of Amorphous Semiconductors*, edited by P. G. LeComber and J. Mort (Academic, New York, 1973), Chap. 7.
[15]A Peled and L. B. Schein, Chem. Phys. Lett. **153**, 422 (1988).
[16]P. Sanda, J. Appl. Phys. **64**, 1229 (1988).
[17]C. B. Duke and R. J. Meyer, Phys. Rev. B **23**, 2111 (1981).